

Gate-field control of valley polarization in valleytronics

Ting-Ting Zhang(张婷婷), Yilin Han(韩依琳), Run-Wu Zhang(张闰午), Zhi-Ming Yu(余智明)

Citation: Chin. Phys. B, 2024, 33 (**6**): 067303. DOI: 10.1088/1674-1056/ad401a
Journal homepage: http://cpb.iphy.ac.cn; http://iopscience.iop.org/cpb

What follows is a list of articles you may be interested in

Reanalysis of energy band structure in the type-II quantum wells

Xinxin Li(李欣欣), Zhen Deng(邓震), Yang Jiang(江洋), Chunhua Du(杜春花), Haiqiang Jia(贾海强), Wenxin Wang(王文新), and Hong Chen(陈弘)
Chin. Phys. B, 2024, 33 (**6**): 067302. DOI: 10.1088/1674-1056/ad36bc

Negative magnetoresistance in the antiferromagnetic semimetal $V_{1/3}TaS_2$

Zi Wang(王子), Xin Peng(彭馨), Shengnan Zhang(张胜男), Yahui Su(苏亚慧), Shaodong Lai(赖少东), Xuan Zhou(周旋), Chunxiang Wu(吴春翔), Tingyu Zhou(周霆宇), Hangdong Wang(王杭栋), Jinhu Yang(杨金虎), Bin Chen(陈斌), Huifei Zhai(翟会飞), Quansheng Wu(吴泉生), Jianhua Du(杜建华), Zhiwei Jiao(焦志伟), and Minghu Fang(方明虎)
Chin. Phys. B, 2024, 33 (**3**): 037301. DOI: 10.1088/1674-1056/ad18aa

Gate-controlled localization to delocalization transition of flat band wavefunction in twisted monolayer-bilayer graphene

Siyu Li(李思宇), Zhengwen Wang(王政文), Yucheng Xue(薛禹承), Lu Cao(曹路), Kenji Watanabe, Takashi Taniguchi, Hongjun Gao(高鸿钧), and Jinhai Mao(毛金海)
Chin. Phys. B, 2023, 32 (**6**): 067304. DOI: 10.1088/1674-1056/acc805

Machine learning of the Γ-point gap and flat bands of twisted bilayer graphene at arbitrary angles

Xiaoyi Ma(马宵怡), Yufeng Luo(罗宇峰), Mengke Li(李梦可), Wenyan Jiao(焦文艳), Hongmei Yuan(袁红梅), Huijun Liu(刘惠军), and Ying Fang(方颖)
Chin. Phys. B, 2023, 32 (**5**): 057306. DOI: 10.1088/1674-1056/acb2c3

Spin- and valley-polarized Goos-Hänchen-like shift in ferromagnetic mass graphene junction with circularly polarized light

Mei-Rong Liu(刘美荣), Zheng-Fang Liu(刘正方), Ruo-Long Zhang(张若龙), Xian-Bo Xiao(肖贤波), and Qing-Ping Wu(伍清萍)
Chin. Phys. B, 2023, 32 (**3**): 037301. DOI: 10.1088/1674-1056/ac89e2

TOPICAL REVIEW — Valleytronics

Gate-field control of valley polarization in valleytronics

Ting-Ting Zhang(张婷婷)[1,†], Yilin Han(韩依琳)[2], Run-Wu Zhang(张闰午)[2], and Zhi-Ming Yu(余智明)[2]

[1] *Institute of Physics, Chinese Academy of Sciences, Beijing* 100190, *China*

[2] *Key Laboratory of Advanced Optoelectronic Quantum Architecture and Measurement (MOE), Beijing Key Laboratory of Nanophotonics & Ultrafine Optoelectronic Systems, and School of Physics, Beijing Institute of Technology, Beijing* 100081, *China*

(Received 29 November 2023; revised manuscript received 30 March 2024; accepted manuscript online 18 April 2024)

Valleytronics materials are a kind of special semiconductors which can host multiple symmetry-connected and well-separated electron or hole pockets in the Brillouin zone when the system is slightly n or p doped. Since the low-energy particles residing in these pockets generally are not easily scattered to each other by small perturbations, they are endowed with an additional valley degree of freedom. Analogous to spin, the valley freedom can be used to process information, leading to the concept of valleytronics. The prerequisite for valleytronics is the generation of valley polarization. Thus, a focus in this field is achieving the electric generation of valley polarization, especially the static generation by the gate electric field alone. In this work, we briefly review the latest progress in this research direction, focusing on the concepts of the couplings between valley and layer, i.e., the valley–layer coupling which permits the gate-field control of the valley polarization, the couplings between valley, layer, and spin in magnetic systems, the physical properties, the novel designing schemes for electronic devices, and the material realizations of the gate-controlled valleytronics materials.

Keywords: band structure, electronic transport, optical properties, spintronics

PACS: 73.20.At, 73.23.–b, 78.20.–e, 85.75.–d **DOI:** 10.1088/1674-1056/ad401a

1. Introduction

Valleytronics materials have been attracting broad interest in multiple fields at both fundamental and applied aspects. In these materials, the electronic conduction or valence band exhibits multiple symmetry-connected energy extremal points in the Brillouin zone (BZ).[1–5] With slightly n or p doped, the systems will host multiple electron or hole pockets appearing around the energy extremal points, and the low-energy electrons occupying these pockets are endowed with an additional valley degree of freedom (DoF), as the low-energy particles can maintain their valley index for a long time when the intervalley scattering is absent or weak. Hence, while the valley DoF is an emergent freedom of the low-energy particles, it can be considered as a quantum number to identify the electrons and can be used to encode, store and transfer information, similar to the intrinsic DoF of electrons: spin.[6–20] In view of this, the valley is also termed as a pesudospin. The additional valley DoF leads to the concept of valleytronics in condensed matter physics, referring to the manipulation and application of the electronic valley.[21–37]

The valley DoF can emerge in one-dimensional (1D), 2D and 3D materials. The 2D valleytronics materials may be the most concerned in the field. Compared to their 3D counterparts, the 2D valleytronics materials are flexible and easy to efficiently control by external fields. Moreover, many 2D materials allow for the creation of heterostructures by stacking in different forms and different layers. These heterostructures generally not only maintain the valley DoF of the original monolayers, but also can have unique and required properties by design.[36–45] On the other hand, the physics in 2D systems are more abundant than that in 1D systems. Therefore, it is the discovery and the experimental detection of the 2D valleytronic materials, graphene and transitional metal dichalcogenides (TMDs), that make the field of valleytronics undergo rapid development in the past decade.[46–62]

Since the valley is rooted in the band structure, it naturally inherits the band properties around the valley. When the band properties are opposite for different valleys, one can use them to control the valleys of the low-energy electrons. For example, the TMDs exhibit two inequivalent valleys K and K' located at the corners of the hexagonal BZ. These two valleys are connected by time-reversal symmetry ($\mathcal{T}$), and then have opposite Berry curvatures and orbital magnetic moments. Hence, under an in-plane driving electric field, a sizable valley current appears in the TMDs due to the valley Hall effect.[59,63–72] For TMDs, optical pumping is also an efficient way to control and generate valley polarization, as they have valley-contrasting circular dichroism in the optical interband absorption.[70] For the systems with strong spin–orbit coupling (SOC) effect and without space–time inversion symmetry $\mathcal{PT}$ ($\mathcal{P}$ denotes the spatial inversion symmetry), the valley DoF generally is coupled to spin, such as the case in TMDs. This spin–valley coupling (SVC) effect[70,73–84] provides more diverse methods to control both spin and valley, as the way that can control valley (spin) also can manipulate spin (valley).

[†]Corresponding author. E-mail: ttzhang@iphy.ac.cn

© 2024 Chinese Physical Society and IOP Publishing Ltd

Besides, the 2D materials can be stacked to form 2D heterostructures with two or multiple layers. As a consequence, the 2D systems can exhibit another important DoF, i.e., the layer DoF. The bilayer TMDs with both AA and AB stacking maintain the valley DoF and the SVC effect. And, in addition to layer DoF, the bilayer TMDs exhibit a more varied coupled physics — the coupling between spin, valley, layer and different basis.[59,78,84–87] However, since all the DoFs in the bilayer TMDs are distinguishable, the low-energy effective Hamiltonian that describes the coupled physics is a large matrix with a rank of $2^4 = 16$, which somehow is complicated and not convenient for subsequent analytic calculations.

In this article, we focus on the control and generate valley or spin polarization by gate electric field, which is a crucial task in the fields of valleytronics and spintronics, as the gate field has advantages in compactness, power efficiency, and compatibility with existing semiconductor technology. Since the two valleys in graphene, TMDs and bilayer TMDs are connected by $\mathcal{T}$ symmetry and the gate field does not break $\mathcal{T}$, the valley polarization can not be generated by the gate field in these valleytronics materials. Moreover, even the valleys are not connected by $\mathcal{T}$, they are not necessarily able to be manipulated by the gate field.[29,30,88]

In 2019, Yu *et al.*[89] proposed a new design principle to address this crucial task. In view of symmetry, the new principle is to explore certain systems that (i) the valleys in them are connected by crystalline symmetry $\mathcal{O}$ instead of $\mathcal{T}$ and (ii) $\mathcal{O}$ should be broken by a gate field. Physically, the principle requires the two valleys to have opposite layer polarizations, leading to the valley–layer coupling (VLC). The monolayer Ti_2SiCO_2 (ML-TSCO) is predicted as the first material example with the VLC and efficient gate-control of valley. For a gate field of 0.1 eV/Å, the valley splitting in ML-TSCO reaches 37 meV and 42 meV for valence and conduction bands, respectively.

By combining the VLC and the VSC, a valley-mediated spin–layer coupling (SLC) was proposed by Zhang *et al.*, which allows for the generation of both valley and spin polarizations by a gate field.[90] It was found that this coupling can appear in monolayer $Ca(CoN)_2$.[90] Apparently, the valley-mediated SLC is a special kind of spin–valley–layer coupling that only exists in the systems without $\mathcal{T}$ symmetry and then is completely different from that in bilayer TMDs with $\mathcal{T}$.

In this article, we will briefly review the concepts, the physical consequence, the new design schemes for electronics devices, and the material realizations of the systems with the VLC and valley-mediated SLC. We also present the classification of the valley-related coupling based on the layer polarization in the two valleys, which is the key point for gate-controlled valley polarization. The field of valleytronics is still under rapid development. This short review only provides the readers with the recent progresses in gate-controlled valleytronics (and valley-spintronics) materials. Readers who are interested in the valley physics in graphene and TMDs are suggested to consult the previous articles.[1–4,91–93]

2. Gate-controlled valleytronics

We start by discussing the concept of VLC, which was proposed to realize a gate-field control of valley polarization.[89] The VLC was first proposed for nonmagnetic systems, and later was extended to magnetic systems. In this section, we first review the symmetry requirements for VLC and the valley-mediated SLC, and the classification of the valley related coupling based on physical consequences. Then we discuss the material realization of the gate-controlled valleytronics materials in both nonmagnetic and magnetic systems. Finally, we review several interesting physical properties and device schemes related to these valleytronics materials.

2.1. VLC in nonmagnetic systems

The VLC was first proposed in nonmagnetic material: monolayer Ti_2SiCO_2. Here, we will follow the discussion in Ref. [89]. The 2D materials generally exhibit multiple atomic layers. This means that the layer DoF can be introduced in most of the 2D materials without being stacked, except that the systems contain one single atomic layer, such as graphene.

Specifically, we consider a 2D material that is extended in the x–y plane, and has a finite thickness along z-direction. To introduce a binary layer DoF, without loss of generality we assume that the material consists of two layers: the top layer with $z > 0$ and the bottom layer with $z < 0$, where $z = 0$ is the midpoint of the system along z, as illustrated in Fig. 1(a). From this partition criterion, one knows that both top and bottom layers may contain multiple atomic layers.

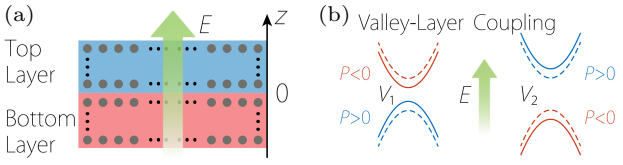


Fig. 1. Illustration of valley–layer coupling: the two valleys have valley-contrasting layer polarization (P). (a) A 2D material system generally can be viewed as two layers. (b) With VLC, an applied gate electrical field can generate valley polarization. The solid (dashed) curves denote the bands in the presence (absence) of the electric field. Reproduced with permission from Ref. [89].

Analogous to spin and valley, we need to define the layer polarization for the discussion of the coupling between layer and other DoFs. According to Ref. [89], the layer polarization of a Bloch band eigenstate $\psi_{n\boldsymbol{k}}(\boldsymbol{r})$ can be defined as

$$P_n(\boldsymbol{k}) = \int_{z>0} |\psi_{n\boldsymbol{k}}(\boldsymbol{r})|^2 \mathrm{d}\boldsymbol{r} - \int_{z<0} |\psi_{n\boldsymbol{k}}(\boldsymbol{r})|^2 \mathrm{d}\boldsymbol{r}, \qquad (1)$$

where n is the band index, $\boldsymbol{k} = (k_x, k_y)$ and $\boldsymbol{r} = (x, y, z)$ denote the momentum in the 2D BZ and the position vector in real space, respectively. Notice that due to the finite thickness of a generic 2D material, the position vector $\boldsymbol{r}$ has also a z component. It is clear that $P_n(\boldsymbol{k}) > 0$ [$P_n(\boldsymbol{k}) < 0$] corresponds to the case that the state $\psi_{n\boldsymbol{k}}(\boldsymbol{r})$ has more weight distributed in the top (bottom) layer. By applying a gate field along z-direction, we immediately know that the states with opposite $P_n(\boldsymbol{k})$ will have opposite energy shifts, as the gate field generates a layer-dependent electrostatic potential. Then if the two valleys have valley-contrasting layer polarizations, i.e., VLC, the electric control of valleys using gate field can be naturally realized, as illustrated in Figs. 1(b) and 2(b).

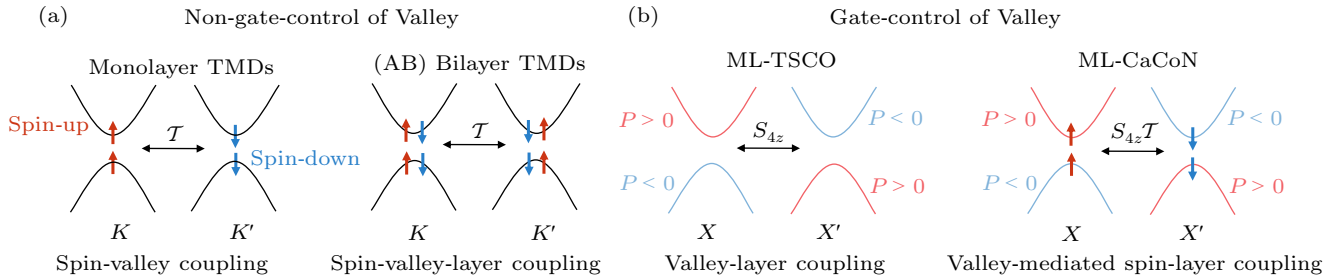


Fig. 2. Illustration of different kinds of spin–valley–layer couplings. (a) The couplings that can not achieve gate control of valley (spin) polarization, as the layer polarizations for the two valleys (spins) are the same, guaranteed by $\mathcal{T}$. (b) The couplings that can achieve gate control of valley polarization. The valley-mediated SLC also can achieve gate control of spin polarization. In these two couplings, the layer polarizations for the two valleys (spins) are the opposite, guaranteed by S_{4z} ($S_{4z}\mathcal{T}$). The red and blue arrows represent spin-up and spin-down, respectively. The black and red (green) curves represent the bands with vanishing and finite layer polarization .

Apparently, the VLC requires symmetry protections for its realization. In Ref. [89], Yu *et al.* discussed the symmetry requirements for nonmagnetic systems with two valleys, denoted as V_1 and V_2. To achieve VLC, the following conditions should be satisfied.[89]

(i) The V_1 and V_2 should form a closed set under all symmetry operations of the system. This means that all the crystal symmetry operations are divided into two parts: $\mathcal{R}$ and $\mathcal{O}$. The V_1 and V_2 are invariant under $\mathcal{O}$ operations and are interchanged under any $\mathcal{R}$ operation,

$$\mathcal{R}V_{1(2)} = V_{2(1)}, \tag{2}$$
$$\mathcal{O}V_{1(2)} = V_{1(2)}. \tag{3}$$

(ii) Since the two valleys must have finite and opposite layer polarizations, $\mathcal{R}$ and $\mathcal{O}$ should satisfy the following relation:

$$\mathcal{R}P(V_{1(2)})\mathcal{R}^{-1} = -P(V_{2(1)}), \tag{4}$$
$$\mathcal{O}P(V_{1(2)})\mathcal{O}^{-1} = P(V_{1(2)}), \tag{5}$$

which is the key symmetry requirement for the VLC.

This symmetry requirement applies to the 2D nonmagnetic system both with and without SOC. It implies that the valleys can not be connected by the symmetry like $\mathcal{T}$, out-of-plane rotation symmetry C_{nz}, and vertical mirrors $M_{x(y)}$, as these symmetries do not reverse the layer polarization. In other word, the symmetries that connect the two valleys should be broken by the gate field. Hence, the V_1 and V_2 must be located at time-reversal-invariant momentum (TRIM) points in nonmagnetic systems. Also, the operations belonging to $\mathcal{O}$ must keep the layer polarization, indicating the spatial inverse symmetry $\mathcal{P}$ and in-plane rotation symmetry $C_{2x(2y)}$ cannot be $\mathcal{O}$ operation. Besides, the horizontal mirror M_z must be broken in the VLC systems, where the layer polarization is suppressed ($P_n = 0$) for all the band states.

Based on these two requirements, one can go through all the 80 layer groups (LGs) or all the 31 layer point groups (LPGs),[94] which describe the group symmetry or the point-group symmetry of the 2D nonmagnetic system with finite thickness, to screen out the ones that allow the existence of VLC. The results are listed in Table 1. There are 5 of the 80 LGs that can host the novel VLC effect, which are LGs 10, 22, 50, 59 and 60. The two valleys appear at TRIM points S and S' for LGs 10 and 22, and at TRIM points X and X' for LGs 50, 59 and 60. This means that for a 2D nonmagnetic material belonging to these LGs, as long as the valleys appear at the target TRIM points, it will exhibit VLC, and is the gate-controlled valleytronics material that we search for.

Table 1. List of the layer groups (LGs) and the corresponding space groups (SGs) that allow for the VLC.[89]

Lattice	(V_1, V_2)	LGs (SGs)
Centered rectangular	(S, S')	10 (5)
		22 (21)
		50 (81)
Square	(X, X')	59 (115)
		60 (117)

2.2. Valley-mediated SLC in magnetic systems

The concept of VLC also can be realized in magnetic systems. Particularly, a recent work[90] shows that the combination of VLC and VSC will lead to a novel spin–valley–layer coupling: valley-mediated SLC, as illustrated in Fig. 2(b). The valley-mediated spin–layer coupling requires the valleys to

exhibit both valley-contrasting spin polarizations and valley-contrasting layer polarizations. If realized, the spin and layer DoFs are coupled, i.e., the spins host spin-contrasting layer polarizations, which according to the definition is the SLC. This valley-mediated SLC naturally enables electric control of both valley and spin by gate field.

Similar to VLC, the valley-mediated SLC requires symmetry protection. Since the gate field does not break $\mathcal{T}$ and the gate-field control of spin polarization can be achieved by the valley-mediated SLC, the 2D system with valley-mediated SLC should be a magnetic material. Following the discussions in Ref. [90], we consider a 2D antiferromagnetic (AM) system without $\mathcal{PT}$ (which is also termed as an altermagnetic system). For simplification, it is assumed that the Néel vector of the 2D AM system is along z-direction, and the system only has two valleys, denoted as V_1 and V_2.[90] The symmetry requirements for the valley-mediated SLC are shown below.[90]

(i) Similarly, the V_1 and V_2 should form a closed set under all symmetry operations of the system. Hence, all the crystal symmetry operations are divided into two parts: $\mathcal{R}$ and $\mathcal{O}$. The V_1 and V_2 are invariant under $\mathcal{O}$ operations and are interchanged under any $\mathcal{R}$ operation, i.e.,

$$\mathcal{R}V_{1(2)} = V_{2(1)}, \tag{6}$$

$$\mathcal{O}V_{1(2)} = V_{1(2)}. \tag{7}$$

(ii) Since the two valleys must have finite and opposite layer and spin polarizations, $\mathcal{R}$ and $\mathcal{O}$ should satisfy the following relation:

$$\mathcal{R}P(V_{1(2)})\mathcal{R}^{-1} = -P(V_{2(1)}), \tag{8}$$

$$\mathcal{O}P(V_{1(2)})\mathcal{O}^{-1} = P(V_{1(2)}) \tag{9}$$

for layer polarization P and

$$\mathcal{R}S_z(V_{1(2)})\mathcal{R}^{-1} = -S_z(V_{2(1)}), \tag{10}$$

$$\mathcal{O}S_z(V_{1(2)})\mathcal{O}^{-1} = S_z(V_{1(2)}) \tag{11}$$

for spin polarization $S_z \equiv \langle \psi_{n\boldsymbol{k}}|\sigma_z|\psi_{n\boldsymbol{k}}\rangle$ with σ_z the Pauli matrix acting on the spin space.

This symmetry requirement also applies to the 2D systems both with and without SOC. Similarly, the symmetries that connect the two valleys here should also be broken by the gate field. Moreover, the valley-mediated SLC requires the operations $\mathcal{R}$ ($\mathcal{O}$) reverse (keep) both spin and layer polarizations of the valleys. As a consequence, the symmetry requirement for the valley-mediated SLC is more rigorous than that for VLC.

The symmetries of the 2D systems with and without SOC are described by magnetic groups and spin groups, respectively. However, as shown in Ref. [90], for the magnetic systems discussed here, it is enough and convenient to use the magnetic groups rather than the complicated spin groups to analyze the SLC in the systems without SOC. Based on the above symmetry requirement, one can conduct a search through all 528 magnetic layer groups (MLGs) to screen out the ones that allow the existence of the valley-mediated SLC. The results are listed in Table 2. There are 23 of the 528 MLGs that can host the valley-mediated SLC. Interestingly, all the five 2D Bravais lattices can host this novel SLC effect. For oblique, rectangular and centered rectangular Bravais lattices, the two valleys are not necessary to appear at high-symmetry points in BZ. However, for square (hexagonal) lattices, the valleys should be located at X (K) and Y (K') points. Again, one knows that for a 2D magnetic material belonging to these MLGs, as long as the valleys appear at the target points, it will exhibit valley-mediated SLC, and is the gate-controlled valleytronics and spintronics material that we are looking for.

Table 2. List of the MLGs and the corresponding magnetic space groups (MSGs) that allow for the valley-mediated SLC. (k,k') denote two generic momentums in the BZ.[90]

Lattice	(V_1, V_2)	MLGs (MSGs)
Oblique	(k, k')	4.3.14 (6.3.27), 5.3.19 (7.3.34)
Rectangular	(k, k')	8.1.34 (3.1.8), 9.1.41 (4.1.15)
	(Σ,Σ')	27.3.156 (25.4.158), 28.3.169 (26.5.172), 29.3.176 (26.5.172), 30.3.183 (27.4.181), 31.3.190 (28.5.189), 32.3.199 (31.5.216), 33.3.204 (29.5.202), 34.3.209 (30.5.209)
Centered rectangular	(k, k')	10.1.45 (5.1.19)
	(S,S')	22.1.122 (21.1.129)
	(x, x')	35.3.214 (38.5.269), 36.3.223 (39.5.282)
Square	(X,Y)	50.3.360 (81.3.695), 59.5.414 (115.3.943), 60.5.421 (117.3.960)
Hexagonal	(K,K')	67.1.467 (149.1.1251)
		74.3.494 (174.3.1365), 78.5.514 (187.3.1441), 79.5.519 (189.3.1453)

2.3. Classification of the couplings in valleytronics

As discussed, the gate-field control of valley and spin is important for valleytronics and spintronics, and the VLC and the valley-mediated SLC provide a simple and transparent way to realize this task. Then, we discuss the difference between the VLC, the valley-mediated SLC and the conventional spin–

layer–valley coupling in bilayer graphene and bilayer TMDs. According to the above symmetry analysis, one knows that the difference is symmetry, as illustrated in Fig. 2.

Analogous to the valley–spin coupling in TMD materials,[70] where the two valleys are connected by a certain symmetry to guarantee their degeneracy in energy and have valley-contrasting spin polarization, the VLC (SLC) is defined as the case that the two symmetry-connected valleys (spins) should have valley-contrasting (spin-contrasting) layer polarization. Since the two valleys in bilayer graphene and bilayer TMDs are connected by $\mathcal{T}$, they must have the same layer polarization, as illustrated in Fig. 2(a). This means that the spin–layer–valley coupling in these bilayer materials is not either the VLC or the valley-mediated SLC. However, for one certain valley, the spin–layer–valley coupling indeed can enable spin polarization by the gate field.

2.4. Material realization

The first example of the VLC material is the nonmagnetic material: monolayer Ti_2SiCO_2.[89] Subsequently, it is found that a number of the TiSiCO-family monolayers Z_2YCO_2 (Z = Ti, Zr, Hf; Y = Si, Ge) also are the VLC materials.[94,95] Figure 3(a) shows the crystalline structure of the ML-TSCO, which possesses five square-lattice atomic layers vertically stacked in the sequence of O–Ti–Si/C–Ti–O. The LG for the ML-TSCO is LG No. 59. The ML-TSCO is both dynamically and thermally stable [see Fig. 3(b)], and its optimized lattice constant is $a = b \approx 2.82$ Å.[89]

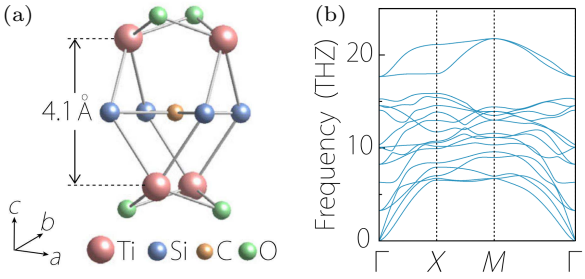


Fig. 3. (a) Crystal structure and (b) phonon spectrum of the ML-TSCO. Reproduced with permission from Ref. [89].

The electronic band structure of the ML-TSCO is presented in Fig. 4(a), from which two valleys appearing at X and X' points can be clearly observed. Hence, according to the above symmetry analysis, one directly knows that the ML-TSCO is a VLC material, namely, the two valleys should have opposite layer polarizations, as guaranteed by the S_{4z} and $C_{2,110}$ symmetries. This is confirmed by the first-principles calculations. By analyzing the spatial distribution of the two valleys, one finds that the conduction band at X (X') valley is mainly distributed in the bottom (top) Ti layer and the valence bands at the two valleys have opposite layer distribution patterns, as shown in Fig. 4(b). Remarkably, the height between the two Ti atoms layers is about 4.1 Å, which is comparable to the interlayer separation for van der Waals stacked heterostructures. Hence, the gate-field control of the valley polarization in ML-TSCO should be very efficient. By applying a gate field , the conduction band at X (X') valley is pulled down (pushed up) and the valence band at X (X') valley is pushed up (pulled down). This successfully generates a valley polarization for either electron or hole carriers when the system is n or p doped. Particularly, for a gate field of 0.1 eV/Å, which is achievable with current experimental technique, the valley splitting respectively reaches 37 meV and 42 meV for valence and conduction bands, which are larger than the thermal energy at room temperature. This means that the ML-TSCO can be used in room-temperature devices.

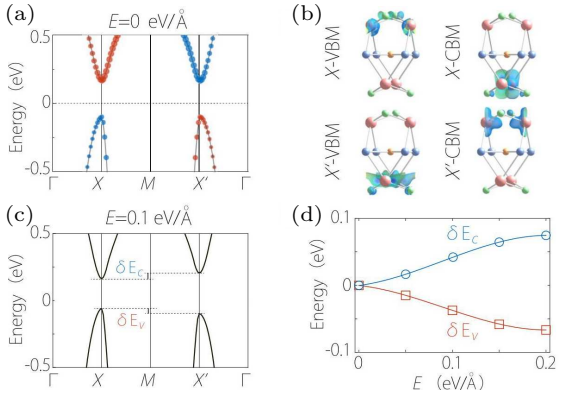


Fig. 4. (a) Electronic band structure of ML-TSCO. The size of the red (blue) dots in (a) is proportional to the weight of projection onto atomic orbital in the bottom (top) Ti atoms. (b) Charge density distribution plotted for VBM and CBM states at the two valleys. (c) The band structure under a gate field of $E = 0.1$ eV/Å. (d) Valley splitting for VBM (δE_v) and CBM (δE_c) [indicated in (c)] versus the applied gate field. Reproduced with permission from Ref. [89].

The first example of the material with valley-mediated SLC is the family of monolayer decorated transition metal nitrides $A(BN)_2$ (A = Mg, Ca, Zn and B = Mn, Fe, Co) materials, which was predicted by Zhang *et al.* very recently.[90] These materials are layered materials that have been demonstrated to be energetically and dynamically stable and may be obtained from their bulk counterpart through mechanical exfoliation. For example, the exfoliation energy for monolayer $Ca(CoN)_2$ (ML-CaCoN) is about 1.19 J/m^2, which is comparable to that of Ca_2N ($\sim$ 1.09 J/m^2)[96] and HfGeTe ($\sim$ 0.98 J/m^2).[97]

Figure 5(a) shows the crystalline structure of the ML-CaCoN, which also possesses five square-lattice atomic layers vertically stacked in the sequence of Co–N–Ca–N–Co. The first-principles calculations show for the ML-CaCoN, the lattice constant is $a = b = 3.55$ Å. The magnetic moments of the ML-CaCoN are mainly on the Co sites with a magnitude of $\sim 3\mu_B$ and the Néel vector is along the z-direction. Hence, in the ground state, the ML-CaCoN belongs to MLG 59.5.414, which is one of the MLG candidates listed in Table 2. In its band structure, one finds that two valleys appear at X and

Y for both valence and conduction bands. Again the above symmetry analysis guarantees that the two valleys should have valley-contrasting spin and layer polarizations. The gate control of valleys and spins in the ML-CaCoN is further demonstrated by calculating the band structure under a vertical electric field. For a gate field of 0.2 eV/Å, the valley and spin splitting in ML-CaCoN reaches 78 meV and 123 meV for valence and conduction bands, respectively.[90] Particularly, the low-energy electrons, i.e., the conduction (valence) bands around the two valleys, feature almost the same energy shift, suggesting an almost uniform, large and static magnetic field of about 10^3 T is generated in ML-CaCoN by a gate field of 0.2 eV/Å. This means that a simple and predictable gate-field control of spin polarization is achieved, which should have a significant impact on the spintronic devices.

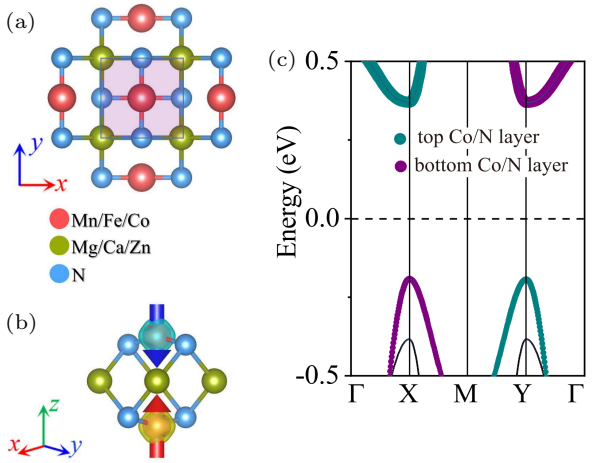


Fig. 5. (a) Top view of the crystal structure of monolayer $A(BN)_2$. The light purple region denotes the primitive cell. (b) Spatial spin-density distribution of ML-CaCoN, showing that the magnetic moments are mainly localized around the top and bottom Co atoms with opposite directions. (c) Orbital-projected band structures, showing that the low-energy bands are mainly contributed by Co and N atoms. Reproduced with permission from Ref. [90].

2.5. Physical properties

A advantage of the valley physics is that it can be described by a low-energy effective Hamiltonian, which is very convenient for theoretical investigations.

For the ML-TSCO, the low-energy physics occur at X and X', both having the little group of C_{2v}. The conduction and valence bands at X (X') valley point correspond to the 1D representations B_2 and A_1 (B_1 and A_1) for the C_{2v} group. Based on these low-energy states, the $k\cdot p$ effective model of the ML-TSCO is established as[89]

$$\mathcal{H}_0 = \Delta\tau_z + v(k_x+k_y)\tau_y - v(k_x-k_y)\sigma_z\tau_y, \tag{12}$$

where the momentum $\boldsymbol{k}$ is measured from each valley point, $\Delta = 0.133$ eV and $v = 0.59$ eV·Å are model parameters that can be obtained by fitting the first-principles results. Here $\sigma_z = \pm 1$ denotes the X (X') valleys, and τ's are Pauli matrices acting on the basis (i.e., the conduction and valence bands) of one valley. Importantly, since the conduction and valence bands have opposite layer polarizations in ML-TSCO, τ can also be regarded as acting on the layer index space. Thus, due to the presence of $\sigma_z\tau_y$ in Eq. (12), one directly knows there is a coupling between valley (σ) and layer (τ) DoFs, which is nothing but the VLC. Moreover, the behavior of the low-energy bands under a gate field is simply captured by

$$\mathcal{H}_E = \Delta_E\sigma_z\tau_z, \tag{13}$$

where the effective energy shift $\Delta_E = \alpha E$ (with $\alpha \approx -0.2$ Å) is a linear function of the gate field (E) when E is not large.

Similarly, the low-energy physics of the valley-mediated SLC in ML-CaCoN can be captured by[90]

$$\mathcal{H} = \Lambda\tau_z + v_1(k_x\tau_x + k_y\tau_y) + v_2(k_x\tau_x - k_y\tau_y)\sigma_z, \tag{14}$$

where $\Lambda = 0.281$ eV, $v_1 = 1.167$ eV·Å and $v_2 = -0.109$ eV·Å, obtained from the first-principles calculations. Again, both σ and τ are Pauli matrices that act on the valley index space and on the basis of one valley, respectively. Similarly, τ can also be regarded as acting on the layer index space. However, in ML-CaCoN, σ can also be considered to operate in the spin space, as both (low-energy) conduction and valence bands at the X (Y) valley are spin-up (spin-down) electrons. Since the last term of Eq. (14) contains $\tau_{x(y)}\sigma_z$, the physics in the ML-CaCoN is not only the VLC but also the valley-mediated SLC. The behavior of the low-energy bands of the ML-CaCoN under a gate field can be easily inferred, and can also be described by Eq. (13). However, since the σ here denotes spin index, the gate field behaves like an uniform magnetic Zeeman field but has opposite signs for conduction and valence bands. For a gate field of $E_z = 0.2$ eV/Å, the induced effective uniform Zeeman fields for conduction and valence bands are about 1.06×10^3 T and -0.67×10^3 T, respectively.

Notice that in ML-TSCO and ML-CaCoN, while there exist three (i.e., valley, layer and basis) and four (i.e., valley, layer, spin and basis) DoFs, the low-energy effective Hamiltonian is not very complex, as some DoFs here are indistinguishable, such as valley and spin in ML-CaCoN [see Fig. 2(b)].

With these effective Hamiltonians, we are able to theoretically study various physical properties of the systems with VLC or valley-mediated SLC. One of the interesting physical properties is the optical phenomena. For example, one can study the optical interband absorption from the effective Hamiltonian. The coupling strength with optical fields linearly polarized in the x (y) direction is given by[89]

$$M_{x(y)}(\boldsymbol{k}) \sim \langle u_c(\boldsymbol{k})|\frac{\partial\mathcal{H}}{\partial k_{x(y)}}|u_v(\boldsymbol{k})\rangle, \tag{15}$$

where $u_{c(v)}$ is the periodic part of the Bloch state of the conduction (valence) band. From the effective Hamiltonian (12)

of the ML-TSCO, one finds that for the X valley,[89]

$$|M_x^X(\boldsymbol{k})|^2 = O(k^2), \quad |M_y^X(\boldsymbol{k})|^2 = \frac{4v^2 m_e^2 \Delta^2}{4v^2 k_y^2 + \Delta^2}. \tag{16}$$

Similarly, for the X' valley, one has

$$M_{x/y}^{X'}(k_x, k_y) = M_{y/x}^{X}(-k_y, k_x). \tag{17}$$

Thus, the interband transitions around the X' (X) valley point are coupled exclusively with x-linearly (y-linearly) polarized light, as shown in Fig. 6(a). This valley linear dichroism can also be understood by the symmetry, as the two valleys in ML-TSCO belong to the C_{2v} point group and are connected by S_{4z}. For the ML-CaCoN, it will exhibit valley- and spin-contrasting elliptical dichroism, namely, the interband transitions around the two valleys are coupled exclusively with left and right elliptically polarized light.[90] These properties mean that we can selectively excite carriers in one valley by controlling the polarization of light in both ML-TSCO and ML-CaCoN. Further applying a gate electric field will not affect the dichroism, but can tune the position of the absorption peaks.

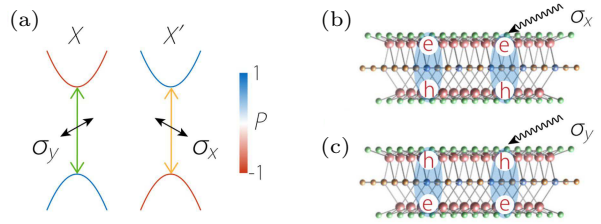


Fig. 6. (a) Valley-contrasting optical transition selection rules in ML-TSCO. (b) and (c) Interlayer excitons with valley-contrasting layer polarization. Reproduced with permission from Ref. [89].

More interestingly, since the conduction and valence bands at one particular valley of both ML-TSCO and ML - CaCoN have opposite layer polarizations, the optically excited electrons and holes are located at different layers. Consequently, the interaction between the electrons and holes will lead to the formation of interlayer excitons with valley-contrasting layer polarization, as illustrated in Fig. 6(b). For the ML-TSCO, the x-polarized light with suitable frequency will selectively generate excitons in the X' valley, in which the holes are located in the top layer and the electrons are located in the bottom layer. These interlayer excitons naturally carry a charge polarization along z, which provides a possibility to manipulate the excitons by electric method even though the excitons are charge neutral. Similarly, the excitons in the ML-CaCoN also are interlayer excitons with valley-contrasting layer polarization and spin polarization.

Another interesting phenomenon is that the VLC and the valley-mediated SLC can permit the design of novel valleytronics and spintronics devices.[89,90] As discussed in Ref. [89], the gate-controlled valleytronics materials, such as the ML-TSCO, allow us to write in and read off the valley information by purely electric means. This effect applies to both non-magnetic and magnetic materials. The fully electric manipulation of valley makes the gate-controlled valleytronics materials have great advantage in producing qubits and designing energy-efficient electronics. One also can use the ML-CaCoN alone to realize the device like tunneling magnetoresistance (TMR) devices without resorting to magnetic field,[90] as depicted in Fig. 7. For n doped ML-CaCoN, when the gate fields at the left and right terminals are the same, the system will have a low resistance. In contrast, for the antiparallel configuration, i.e., the gate fields at the left and right terminals are the opposite, the electrons moving from left to right must switch spin, valley and layer indexes, indicating that the transitions would be extremely less probable during the transport. Hence, the system under antiparallel configuration will have a very high resistance. One can expect that the TMR effect here should be more pronounced than that in conventional TMR devices, where only the spin index is changed in the transport with antiparallel configuration.

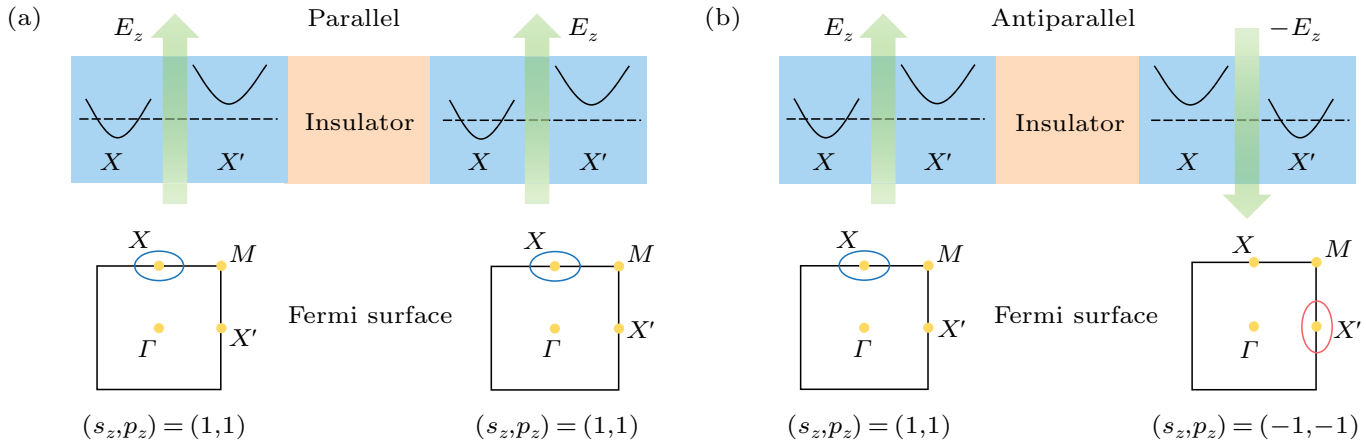


Fig. 7. Illustration of TMR-like device based on the materials with VLC and valley-mediated SLC.[90] (a) Parallel and (b) antiparallel configurations of the TMR-like device under a gate field rather than a magnetic field. Top (bottom) row shows the band structure (Fermi surface) under an external gate field. s_z (p_z) denotes the spin (layer) index.

2.6. VLC and SLC in stacked materials

In addition to stable and intrinsic materials like ML-TSCO and ML-CaCoN, one can also utilize stacking engineering to achieve systems with VLC or valley-mediated SLC in bilayer materials, owing to the stackability of the 2D system.

Recently, Tong *et al.*[68] introduced the concept of ferrovalley and predicted monolayer 2H-VSe_2 as such ferrovalley material. Monolayer 2H-VSe_2 possesses a hexagonal structure but lacks $\mathcal{P}$ and $\mathcal{T}$ symmetries. It exhibits two valleys at the two inequivalent K points, which however are non-degenerate in energy, leading to intrinsic valley polarization, i.e., the ferrovalley state, as shown in Fig. 8. Additionally, the valley polarization in monolayer 2H-VSe_2 strongly depends on the magnetic moment. Reversing the magnetic moment switches the valley polarization from the K_+ to K_- valley (see Fig. 8). Similar situation can also be found in AA′ stacked bilayer VSi_2N_4, which has interlayer antiferromagnetic coupling and is the most stable state for bilayer VSi_2N_4.[98] The AA′ stacked bilayer VSi_2N_4 is a ferrovalley material with two valleys appearing at K_+ to K_- valley, and its valley polarization can also be switched by reversing the magnetic moment in both layers. However, unlike monolayer 2H-VSe_2, the valley state here is spin-degenerate due to the presence of $\mathcal{PT}$ symmetry. Notably, the metastable state of bilayer VSi_2N_4, i.e., ferromagnetic VSi_2N_4, is a ferromagnetic VLC material.[98] Besides, the monolayer Co_2CF_2 is also a magnetic ferrovalley material.[99]

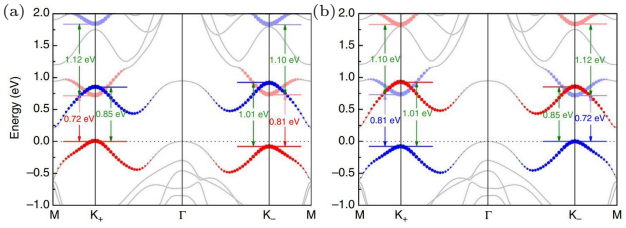


Fig. 8. The band structure of monolayer 2H-VSe_2 with magnetism and SOC effect. (a) and (b) have opposite magnetic moments. Red and blue denote spin-up and spin-down, respectively. Reproduced with permission from Ref. [68].

Based on the concept of ferrovalley, a possible approach to designing materials with VLC or valley-mediated SLC is to stack ferrovalley materials in a suitable manner. Take monolayer 2H-VSe_2 as an example. If we stack two 2H-VSe_2 monolayers with opposite magnetic moments in AA′ form (the band structures of the two monolayers are shown in Fig. 8), one might anticipate that this bilayer material would exhibit two energy-degenerate valleys at the K_+ and K_- points. Specifically, the electronic state of the valence band maximum at K_+ valley would be spin-up and primarily distributed in one certain layer, while that at K_- valley would be spin-down and mainly originate from the other layer. Consequently, such a bilayer system could potentially yield a system with both VLC and valley-mediated SLC effects. However, as depicted in Fig. 8, one can observe that the energy difference between the bands at the Γ and $K_\pm$ points is small. Thus, for the bilayer 2H-VSe_2 discussed here, the physics associated with VLC and valley-mediated SLC may be affected by the bands around the Γ point.

Via symmetry analysis, Xu *et al.*[100] investigated the possibility of achieving VLC materials in non-magnetic systems with orthorhombic lattice through stacking engineering. Consider a 2D orthorhombic material with C_{2z} symmetry and spatial inversion $\mathcal{P}$. Its electronic states are anisotropic along the x and y directions due to the presence of only orthorhombic symmetry, and are required to possess a valley at either the X or Y point. This material can have a single atomic layer or multiple atomic layers. If the difference between the lattice constants along the x and y directions of this material is not significant, a slight strain can be employed to reshape this orthorhombic material into a square configuration. A bilayer system can be constructed by stacking this strained 2D material in AB form, where the top monolayer is rotated 90° around the z-axis compared to the bottom monolayer. The obtained bilayer lattice can possess S_4 symmetry and falls into one of the target layer groups listed in Ref. [89]. Additionally, it can be expected that this stacked material will have two valleys at both X and Y points, contributed respectively by the top and bottom layers. Consequently, a VLC system is established through stacking engineering. Based on symmetry analysis, Xu *et al.*[100] identified 8 out of 80 layer groups that allow for constructing such a bilayer lattice with VLC, which are SGs 47, 50, 51, 53, 55, 59, 65, and 67.

Furthermore, Xu *et al.*[100] demonstrated their idea via first-principle calculations in AB stacked MnF_4 and $TaOI_2$. Let us consider the monolayer MnF_4 as an example to illustrate the processes proposed by Xu *et al.*[100] The monolayer MnF_4 exhibits a low exfoliation energy and can be feasibly obtained experimentally from its $P2_1/c$ bulk phase. It possesses *pman* symmetry (SG 53), which is one of the candidate groups mentioned earlier. The electronic band structures of the monolayer MnF_4 and the rotated monolayer MnF_4 are depicted in Figs. 9(a) and 9(b), respectively. Notably, for the valence bands, these materials respectively exhibit valleys at the X and Y points. Xu *et al.*[100] initially subjected these two monolayers to a slight strain to achieve a square shape, following which they vertically stacked them together to form a bilayer system. The electronic band structure of the resulting bilayer MnF_4 is shown in Fig. 9(c), where two valleys at the X and Y points are clearly observable. Given that the bilayer MnF_4 possesses S_{4z} symmetry, the two valleys must exhibit valley-contrasted layer polarization. This example directly illustrates that a VLC material or valley-mediated SLC material can indeed be realized by stacking ferrovalley materials in a suitable manner.

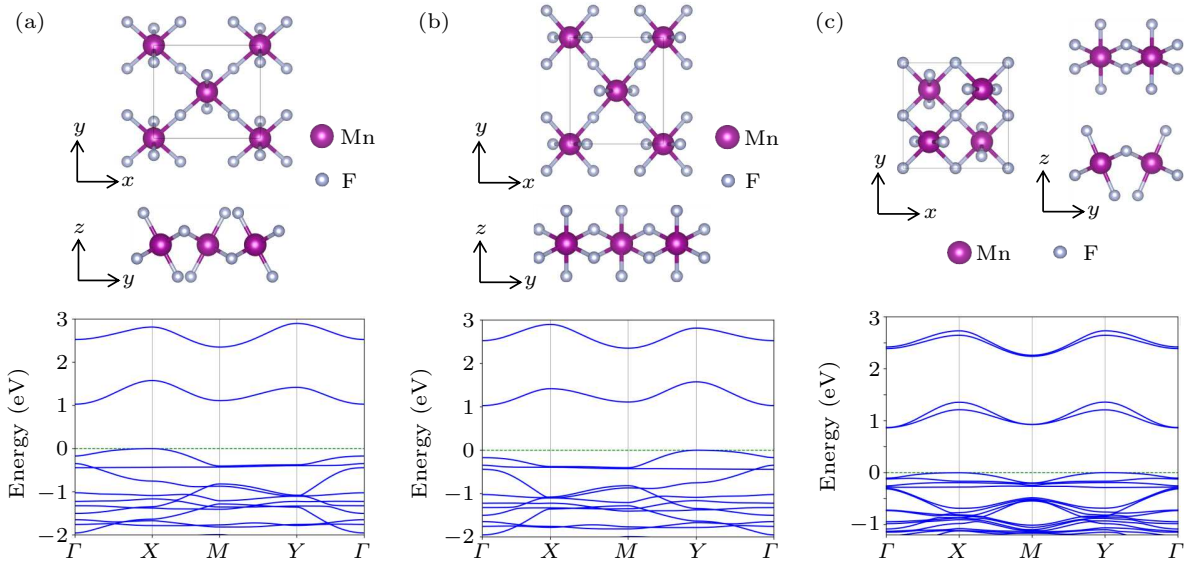


Fig. 9. Crystal and band structures of (a) the monolayer, (b) the rotated monolayer, and (c) the AB stacked bilayer MnF_4.[100] For the bilayer MnF_4, a small strain is applied to both top and bottom layers to make them have a square shape.

3. Summary and outlook

In this article, we have provided a brief overview of the concepts of VLC and valley-mediated SLC, along with their potential applications in gate-controlled valleytronics and spintronics. The future development of valleytronics holds promise for various advancements, including quantum information processing utilizing valley DoF, energy-efficient electronic devices via the valley currents, and the development of photodetectors and light-emitting diodes based on valley dichroism. VLC and SLC materials offer a fertile ground for exploring fundamental physics and designing novel devices that align with existing semiconductor technologies.

Looking ahead, several interesting questions and directions deserve further exploration.

Firstly, the scarcity of suitable materials for VLC and valley-mediated SLC poses a significant challenge. It is imperative to search for and design more suitable material candidates. This can be approached through two main avenues: exploring intrinsic materials that naturally host VLC and valley-mediated SLC, such as ML-TSCO and ML-CaCoN, and employing stacking engineering techniques. For stacking engineering, the study conducted in Ref. [100] only considers 2D orthorhombic materials for realizing VLC materials. Thus, it is urgent to present a systematic investigation into stacking engineering to realize both VLC materials and valley-mediated SLC materials.

Secondly, extending the study of VLC to magnetic systems, such as ferromagnetic and antiferromagnetic systems with the Néel vector pointing along generic directions, could yield promising results. This expansion could significantly increase the number of target groups that allow for the existence of VLC, thereby broadening the range of candidate materials. The introduction of magnetism may also introduce richer physics into VLC materials.

Finally, further exploration of the physical properties of these novel materials, particularly the interplay between binary DoF (such as valley and layer) and external fields, is needed. This includes systematic studies on electric, magnetic, optical, and transport properties that can be efficiently controlled by gate fields in valleytronics materials. These investigations will deepen our understanding of VLC and SLC materials and pave the way for their practical applications in the next-generation electronic and optoelectronic devices.

Acknowledgments

Project supported by the National Natural Science Foundation of China (Grant No. 12004035) and the National Natural Science Fund for Excellent Young Scientists Fund Program (Overseas).

References

[1] Schaibley J R, Yu H, Clark G, Rivera P, Ross J S, Seyler K L, Yao W and Xu X 2016 *Nature Reviews Materials* **1** 16055
[2] Vitale S A, Nezich D, Varghese J O, Kim P, Gedik N, Jarillo-Herrero P, Xiao D and Rothschild M 2018 *Small* **14** 1801483
[3] Xin J, Tang Y, Liu Y, Zhao X, Pan H and Zhu T 2018 *npj Quantum Materials* **3** 9
[4] Liu Y, Gao Y, Zhang S, He J, Yu J and Liu Z 2019 *Nano Research* **12** 2695
[5] Tian H, Ren C and Wang S 2022 *Nanotechnology* **33** 212001
[6] Awschalom D D and Flatté M E 2007 *Nat. Phys.* **3** 153
[7] Bader S and Parkin S 2010 *Annual Review of Condensed Matter Physics* **1** 71
[8] Baltz V, Manchon A, Tsoi M, Moriyama T, Ono T and Tserkovnyak Y 2018 *Rev. Mod. Phys.* **90** 015005
[9] Chappert C, Fert A and Van Dau F N 2007 *Nat. Mater.* **6** 813
[10] Cheng L, Wang X, Yang W, Chai J, Yang M, Chen M, Wu Y, Chen X, Chi D, Goh K E J, Zhu J X, Sun H, Wang S, Song J C W, Battiato M, Yang H and Chia E E M 2019 *Nat. Phys.* **15** 347

[11] Chumak A V, Vasyuchka V I, Serga A A and Hillebrands B 2015 *Nat. Phys.* **11** 453
[12] Felser C, Fecher G H and Balke B 2007 *Angewandte Chemie International Edition* **46** 668
[13] Feng Y P, Shen L, Yang M, Wang A, Zeng M, Wu Q, Chintalapati S and Chang C R 2017 *WIREs Computational Molecular Science* **7** e1313
[14] Han W, Kawakami R K, Gmitra M and Fabian J 2014 *Nat. Nanotechnol.* **9** 794
[15] Li M, Zhang D, Gao Y, Cao C and Long M 2017 *Organic Electronics* **44** 168
[16] Parkin S S P, Hayashi M and Thomas L 2008 *Science* **320** 190
[17] Roche S, Åkerman J, Beschoten B, Charlier J C, Chshiev M, Dash S P, Dlubak B, Fabian J, Fert A, Guimarães M, Guinea F, Grigorieva I, Schönenberger C, Seneor P, Stampfer C, Valenzuela S O, Waintal X and van Wees B 2015 *2D Materials* **2** 030202
[18] Wolf S A, Awschalom D D, Buhrman R A, Daughton J M, von Molnár S, Roukes M L, Chtchelkanova A Y and Treger D M 2001 *Science* **294** 1488
[19] Wunderlich J, Park B G, Irvine A C, Zârbo L P, Rozkotová E, Nemec P, Novák V, Sinova J and Jungwirth T 2010 *Science* **330** 1801
[20] Zutić I, Fabian J and Das Sarma S 2004 *Rev. Mod. Phys.* **76** 323
[21] Gunawan O, Shkolnikov Y P, Vakili K, Gokmen T, De Poortere E P and Shayegan M 2006 *Phys. Rev. Lett.* **97** 186404
[22] Li J, Zhang R X, Yin Z, Zhang J, Watanabe K, Taniguchi T, Liu C and Zhu J 2018 *Science* **362** 1149
[23] Pan H, Li X, Zhang F and Yang S A 2015 *Phys. Rev. B* **92** 041404
[24] Pan H, Li X, Jiang H, Yao Y and Yang S A 2015 *Phys. Rev. B* **91** 045404
[25] Qiao Z, Jung J, Lin C, Ren Y, MacDonald A H and Niu Q 2014 *Phys. Rev. Lett.* **112** 206601
[26] Shkolnikov Y P, De Poortere E P, Tutuc E and Shayegan M 2002 *Phys. Rev. Lett.* **89** 226805
[27] Vitale S A, Nezich D, Varghese J O, Kim P, Gedik N, Jarillo-Herrero P, Xiao D and Rothschild M 2018 *Small* **14** 1801483
[28] Xiao D, Chang M C and Niu Q 2010 *Rev. Mod. Phys.* **82** 1959
[29] Chen C, Chen X, Shao Y, Deng B, Guo Q, Ma C and Xia F 2018 *ACS Photonics* **5** 3814
[30] Rodin A S, Gomes L C, Carvalho A and Castro Neto A H 2016 *Phys. Rev. B* **93** 045431
[31] Beyer H, Rohde G, Grubišić Čabo A, Stange A, Jacobsen T, Bignardi L, Lizzit D, Lacovig P, Sanders C E, Lizzit S, Rossnagel K, Hofmann P and Bauer M 2019 *Phys. Rev. Lett.* **123** 236802
[32] Ingla-Aynés J, Herling F, Fabian J, Hueso L E and Casanova F 2021 *Phys. Rev. Lett.* **127** 047202
[33] Norden T, Zhao C, Zhang P, Sabirianov R, Petrou A and Zeng H 2019 *Nat. Commun.* **10** 4163
[34] Pisoni R, Davatz T, Watanabe K, Taniguchi T, Ihn T and Ensslin K 2019 *Phys. Rev. Lett.* **123** 117702
[35] Zhang X, Hu R Z, Li H O, Jing F M, Zhou Y, Ma R L, Ni M, Luo G, Cao G, Wang G L, Hu X, Jiang H W, Guo G C and Guo G P 2020 *Phys. Rev. Lett.* **124** 257701
[36] Scuri G, Andersen T I, Zhou Y, Wild D S, Sung J, Gelly R J, Bérubé D, Heo H, Shao L, Joe A Y, Mier Valdivia A M, Taniguchi T, Watanabe K, Lončar M, Kim P, Lukin M D and Park H 2020 *Phys. Rev. Lett.* **124** 217403
[37] Zhang H, Yang W, Ning Y and Xu X 2020 *Phys. Rev. B* **101** 205404
[38] Dankert A and Dash S P 2017 *Nat. Commun.* **8** 16093
[39] Dong X J, Jia K, Ji W X, Li S S and Zhang C W 2023 *ACS Applied Electronic Materials* **5** 2046
[40] Gurram M, Omar S and van Wees B J 2018 *2D Materials* **5** 032004
[41] Hidalgo-Sacoto R, Gonzalez R I, Vogel E E, Allende S, Mella J D, Cardenas C, Troncoso R E and Munoz F 2020 *Phys. Rev. B* **101** 205425
[42] Hu T, Zhao G, Gao H, Wu Y, Hong J, Stroppa A and Ren W 2020 *Phys. Rev. B* **101** 125401
[43] Li Q, Chen K Q and Tang L M 2020 *Phys. Rev. Appl.* **13** 014064
[44] Ma X, Shao X, Fan Y, Liu J, Feng X, Sun L and Zhao M 2020 *Journal of Materials Chemistry C* **8** 14895
[45] Wang M, Zhou W, Bi L, Qiu C, Ke M and Liu Z 2020 *Nat. Commun.* **11** 3000
[46] Edwards B, Dowinton O, Hall A E, Murgatroyd P A E, Buchberger S, Antonelli T, Siemann G R, Rajan A, Morales E A, Zivanovic A, Bigi C, Belosludov R V, Polley C M, Carbone D, Mayoh D A, Balakrishnan G, Bahramy M S and King P D C 2023 *Nat. Mater.* **22** 459
[47] Akhmerov A R, Bardarson J H, Rycerz A and Beenakker C W J 2008 *Phys. Rev. B* **77** 205416
[48] Cheng S g, Liu H, Jiang H, Sun Q F and Xie X C 2018 *Phys. Rev. Lett.* **121** 156801
[49] Cresti A, Grosso G and Parravicini G P 2008 *Phys. Rev. B* **77** 233402
[50] Garcia-Pomar J L, Cortijo A and Nieto-Vesperinas M 2008 *Phys. Rev. Lett.* **100** 236801
[51] Grujić M M, Tadić M Ž and Peeters F M 2014 *Phys. Rev. Lett.* **113** 046601
[52] Gunlycke D and White C T 2011 *Phys. Rev. Lett.* **106** 136806
[53] Jiang Y, Low T, Chang K, Katsnelson M I and Guinea F 2013 *Phys. Rev. Lett.* **110** 046601
[54] Nguyen V H, Dechamps S, Dollfus P and Charlier J C 2016 *Phys. Rev. Lett.* **117** 247702
[55] Niu Q, Chang M C, Wu B, Xiao D and Cheng R 2017 *Physical Effects of Geometric Phases* (World Scientific)
[56] Rycerz A, Tworzydło J and Beenakker C W J 2007 *Nat. Phys.* **3** 172
[57] Settnes M, Power S R, Brandbyge M and Jauho A P 2016 *Phys. Rev. Lett.* **117** 276801
[58] Liu G B, Xiao D, Yao Y, Xu X and Yao W 2015 *Chemical Society Reviews* **44** 2643
[59] Sui M, Chen G, Ma L, Shan W Y, Tian D, Watanabe K, Taniguchi T, Jin X, Yao W, Xiao D and Zhang Y 2015 *Nat. Phys.* **11** 1027
[60] Huang Z, Xian G, Xiao X, Han X, Qian G, Shen C, Yang H, Chen H, Liu B, Wang Z and Gao H J 2023 *Nano Lett.* **23** 3274
[61] Lu J, Bao D L, Qian K, Zhang S, Chen H, Lin X, Du S X and Gao H J 2017 *ACS Nano* **11** 1689
[62] Wang Y, Li L, Yao W, Song S, Sun J T, Pan J, Ren X, Li C, Okunishi E, Wang Y Q, Wang E, Shao Y, Zhang Y Y, Yang H t, Schwier E F, Iwasawa H, Shimada K, Taniguchi M, Cheng Z, Zhou S, Du S, Pennycook S J, Pantelides S T and Gao H J 2015 *Nano Lett.* **15** 4013
[63] Gorbachev R V, Song J C W, Yu G L, Kretinin A V, Withers F, Cao Y, Mishchenko A, Grigorieva I V, Novoselov K S, Levitov L S and Geim A K 2014 *Science* **346** 448
[64] Hu H, Tong W Y, Shen Y H, Wan X and Duan C G 2020 *npj Computational Materials* **6** 129
[65] Lee J, Mak K F and Shan J 2016 *Nat. Nanotechnol.* **11** 421
[66] Mak K F, McGill K L, Park J and McEuen P L 2014 *Science* **344** 1489
[67] Shimazaki Y, Yamamoto M, Borzenets I V, Watanabe K, Taniguchi T and Tarucha S 2015 *Nat. Phys.* **11** 1032
[68] Tong W Y, Gong S J, Wan X and Duan C G 2016 *Nat. Commun.* **7** 13612
[69] Xiao D, Yao W and Niu Q 2007 *Phys. Rev. Lett.* **99** 236809
[70] Xiao D, Liu G B, Feng W, Xu X and Yao W 2012 *Phys. Rev. Lett.* **108** 196802
[71] Glazov M M and Golub L E 2020 *Phys. Rev. Lett.* **125** 157403
[72] Cysne T P, Costa M, Canonico L M, Nardelli M B, Muniz R B and Rappoport T G 2021 *Phys. Rev. Lett.* **126** 056601
[73] Cui Q, Zhu Y, Liang J, Cui P and Yang H 2021 *Phys. Rev. B* **103** 085421
[74] Gong Z, Liu G B, Yu H, Xiao D, Cui X, Xu X and Yao W 2013 *Nat. Commun.* **4** 2053
[75] Lin L, Xu Y, Zhang S, Ross I M, Ong A C M and Allwood D A 2013 *ACS Nano* **7** 8214
[76] Liu G B, Xiao D, Yao Y, Xu X and Yao W 2015 *Chemical Society Reviews* **44** 2643
[77] Pisoni R, Kormányos A, Brooks M, Lei Z, Back P, Eich M, Overweg H, Lee Y, Rickhaus P, Watanabe K, Taniguchi T, Imamoglu A, Burkard G, Ihn T and Ensslin K 2018 *Phys. Rev. Lett.* **121** 247701
[78] Xu X, Yao W, Xiao D and Heinz T F 2014 *Nat. Phys.* **10** 343
[79] Yuan H, Wang X, Lian B, Zhang H, Fang X, Shen B, Xu G, Xu Y, Zhang S C, Hwang H Y and Cui Y 2014 *Nat. Nanotechnol.* **9** 851
[80] Zeng H, Liu G B, Dai J, Yan Y, Zhu B, He R, Xie L, Xu S, Chen X, Yao W and Cui X 2013 *Scientific Reports* **3** 1608
[81] Ai H, Liu D, Geng J, Wang S, Lo K H and Pan H 2021 *Physical Chemistry Chemical Physics* **23** 3144
[82] Zhao J, Yang C, Yuan W, Zhang D, Long Y, Pan Y, Chen H, Zhong Z and Ren J 2022 *Phys. Rev. Lett.* **129** 275501
[83] Cai X, Connors E J, Edge L F and Nichol J M 2023 *Nat. Phys.* **19** 386
[84] Jones A M, Yu H, Ross J S, Klement P, Ghimire N J, Yan J, Mandrus D G, Yao W and Xu X 2014 *Nat. Phys.* **10** 130
[85] Qiao Z, Jung J, Niu Q and MacDonald A H 2011 *Nano Lett.* **11** 3453

[86] San-Jose P, Prada E, McCann E and Schomerus H 2009 *Phys. Rev. Lett.* **102** 247204

[87] Ju L, Shi Z, Nair N, Lv Y, Jin C, Velasco J, Ojeda-Aristizabal C, Bechtel H A, Martin M C, Zettl A, Analytis J and Wang F 2015 *Nature* **520** 650

[88] Hanakata P Z, Carvalho A, Campbell D K and Park H S 2016 *Phys. Rev. B* **94** 035304

[89] Yu Z M, Guan S, Sheng X L, Gao W and Yang S A 2020 *Phys. Rev. Lett.* **124** 037701

[90] Zhang R W, Cui C, Li R, Duan J, Li L, Yu Z M and Yao Y 2023 arXiv:2306.08902 [physics.app-ph]

[91] Wang G, Chernikov A, Glazov M M, Heinz T F, Marie X, Amand T and Urbaszek B 2018 *Rev. Mod. Phys.* **90** 021001

[92] Xu X, Yao W, Xiao D and Heinz T F 2014 *Nat. Phys.* **10** 343

[93] Zhao S, Li X, Dong B, Wang H, Wang H, Zhang Y, Han Z and Zhang H 2021 *Reports on Progress in Physics* **84** 026401

[94] Han Y, Cui C, Li X P, Zhang Z, Yu Z M and Yao Y 2024 arXiv:2306.08384 [cond-mat.mes-hall]

[95] Cui C, Han Y, Zhang T T, Yu Z M and Yao Y 2023 *Phys. Rev. B* **108** 155115

[96] Zhao S, Li Z and Yang J 2014 *J. Am. Chem. Soc.* **136** 13313

[97] Guan S, Liu Y, Yu Z M, Wang S S, Yao Y and Yang S A 2017 *Phys. Rev. Mater.* **1** 054003

[98] Liang L, Yang Y, Wang X and Li X 2023 *Nano Lett.* **23** 858

[99] Wang H, Liang L, Wang X, Wang X and Li X 2024 *Appl. Phys. Lett.* **124** 092906

[100] Xu X, He Z, Dai Y, Huang B, Kou L and Ma Y 2021 *Appl. Phys. Lett.* **119** 073101